

Sequential Interactions of Structural Proteins in Phage ϕ 29 Procapsid Assembly

CHOONG-SIK LEE† AND PEIXUAN GUO*

Department of Pathobiology and Purdue Biochemistry & Molecular Biology Program,
Purdue University, West Lafayette, Indiana 47907

Received 15 February 1995/Accepted 5 May 1995

The mechanism of viral capsid assembly is an intriguing problem because of its fundamental importance to research on synthetic viral particle vaccines, gene delivery systems, antiviral drugs, chimeric viruses displaying antigens or ligands, and the study of macromolecular interactions. The genes coding for the scaffolding (gp7), capsid (gp8), and portal vertex (gp10) proteins of the procapsid of bacteriophage ϕ 29 of *Bacillus subtilis* were expressed in *Escherichia coli* individually or in combination to study the mechanism of ϕ 29 procapsid assembly. When expressed alone, gp7 existed as a soluble monomer, gp8 aggregated into inclusion bodies, and gp10 formed the portal vertex. Circular dichroism spectrum analysis indicated that gp7 is mainly composed of α helices. When two of the proteins were coexpressed, gp7 and gp8 assembled into procapsid-like particles with variable sizes and shapes, gp7 and gp10 formed unstable complexes, and gp8 and gp10 did not interact. These results suggested that gp7 served as a bridge for gp8 and gp10. When gp7, gp8, and gp10 were coexpressed, active procapsids were produced. Complementation of extracts containing one or two structural components could not produce active procapsids, indicating that no stable intermediates were formed. A dimeric gp7 concatamer promoted the solubility of gp8 but was inactive in the assembly of procapsid or procapsid-like particles. Mutation at the C terminus of gp7 prevented it from interacting with gp8, indicating that this part of gp7 may be important for interaction with gp8. Coexpression of the portal protein (gp20) of phage T4 with ϕ 29 gp7 and gp8 revealed the lack of interaction between T4 gp20 and ϕ 29 gp7 and/or gp8. Perturbing the ratio of the three structural proteins by duplicating one or another gene did not reduce the yield of potentially infectious particles. Changing of the order of gene arrangement in plasmids did not affect the formation of active procapsids significantly. These results indicate that ϕ 29 procapsid assembly deviated from the single-assembly pathway and that coexistence of all three components with a threshold concentration was required for procapsid assembly. The trimolecular interaction was so rapid that no true intermediates could be isolated. This finding is in accord with the result of capsid assembly obtained by the equilibrium model proposed by A. Zlotnick (J. Mol. Biol. 241:59–67, 1994).

The mechanism of viral capsid assembly has attracted increasing attention because of its fundamental importance to research on the development of synthetic viral particle vaccines (14–15b), the construction of in vivo gene delivery systems, the design of antiviral drugs, the assembly of chimeric viruses displaying antigenic determinants or ligands, and the study of macromolecular interactions. The assembly of viral capsids with multiple copies of protein subunits is analogous to the process of constructing buildings, of various shapes and sizes, with uniform building blocks. In constructing a building, it is the site engineer who controls how particular blocks are assembled into a defined structure. Beyond the principle of quasi-equivalence, the mechanism that controls the assembly of capsids with an elongated (prolate) shape, such as phages T4 and ϕ 29, from uniform subunits is still unknown (14, 27).

There are common features of morphogenesis among the double-stranded DNA viruses. Commonality includes the use of a noncapsid enzyme(s) to translocate the viral DNA into a preassembled protein shell called procapsid (1, 4, 7, 9, 15b, 22, 31). In double-stranded DNA bacteriophages, the procapsids are minimally composed of three structural components: the

scaffolding, capsid, and portal vertex proteins (1, 2, 7, 9). The shape and size of the procapsid are determined by these three proteins (7, 24, 27).

The data accumulated from the study of phage assembly have led to the conclusion that most macromolecular assembly follows a well-defined single-assembly pathway (7). In the single-assembly pathway, if the particle ABC is composed of components A, B, and C, and the assembly pathway is $A + B \rightarrow AB + C \rightarrow ABC$, then the interactions and reactions between A and C and between B and C cannot occur. This is particularly true in phage T4 tail assembly (7, 8a, 28–30). However, it has been difficult to interpret the mechanism of procapsid assembly by the single-assembly pathway (1, 27).

The portal vertex was postulated to be the initiator of phage P22 procapsid assembly (36), but the scaffolding and capsid proteins of P22 were polymerized efficiently into particles in vivo and in vitro without portal vertex proteins, indicating that the portal vertex is not required for the initiation of assembly of P22 procapsid-like particles (3, 40). If the scaffolding and capsid proteins interact first during procapsid formation, the portal vertex should be subsequently inserted into the scaffolding-capsid particle. However, the scaffolding and capsid proteins of phage ϕ 29 formed particles of various sizes and shapes in *Escherichia coli* without portal vertex proteins (18). Thus, the portal vertex cannot be inserted into preformed scaffolding-capsid particles, since this will result in procapsids of various sizes and shapes. Also, it has been demonstrated that naked cores of phage T4 (46, 47) and herpes simplex virus (39)

* Corresponding author. Mailing address: B-36 Hansen Life Sciences Research Building, Cancer Research Center, Purdue University, West Lafayette, IN 47907. Phone: (317) 494-7561. Fax: (317) 496-1795. Electronic mail address: guo@vet.purdue.edu.

† Present address: Department of Pathology, Yale University School of Medicine, New Haven, CT 06510.

can be formed without capsid protein. These results eliminate the possibility that the scaffolding-capsid protein complex serves as an initiator in procapsid assembly. Some scientists believe that the portal vertex is involved in the initiation of procapsid assembly, but others have argued that the portal vertex is inserted last into the structure composed of scaffolding and capsid proteins. Therefore, the sequential interactions of structural proteins in procapsid assembly remain an enigma.

The active procapsid of ϕ29 can be composed of only three proteins: the scaffolding protein gp7, the capsid protein gp8, and the portal vertex protein (connector or DNA-translocating vertex) gp10 (1). ϕ29 has a simple procapsid in comparison with that of other phages. The head fiber gp8.5 is dispensable (42). All of the procapsid structural genes are well characterized and have been sequenced (23, 38, 42, 45). When coexpressed from cloned genes in *E. coli*, the three structural proteins assemble into procapsids indistinguishable from native ϕ29 procapsids purified from infected *Bacillus subtilis* cells (18). A small viral RNA (pRNA [p for packaging]) encoded by the ϕ29 genome has a novel and essential role in viral DNA packaging (17). Procapsids produced in *E. coli*, in the absence of ϕ29 pRNA, were fully competent to package ϕ29 DNA in the defined in vitro DNA packaging system (19) by the in vitro addition of cloned and purified pRNA (16, 17, 21, 49, 53, 54). Moreover, these DNA-filled heads were subsequently converted to infectious virions after the addition of neck and tail proteins (19, 32, 33).

Traditionally, suppressor-sensitive mutants of procapsid structural components were used for the studies of procapsid assembly (23, 37, 44). These mutations, still harboring the genes coding for fragments of a structural components, might react atypically with other structural components and interfere with the procapsid assembly. To circumvent this problem and to elucidate the interactions among the procapsid structural components, the genes for the procapsid structural components of phage ϕ29 were cloned individually and in combination in 13 *E. coli* plasmids to study the sequential interactions among these proteins.

MATERIALS AND METHODS

Construction of plasmids for protein expression. To construct plasmid pAR8 (Fig. 1), two oligonucleotides, GP8F and GP8R (Table 1), were used to produce a DNA fragment with the template plasmid pAR7-8-8.5-9-10 (18) by PCR. The resulting DNA fragment contained a gp8 gene, with *NdeI* (from GP8F) and *BamHI* (from GP8R) restriction sites at the 5' and 3' ends, respectively. This DNA fragment was inserted into *NdeI*-*BamHI* sites of the expression plasmid pET3c/EV (33) (Fig. 1), which was derived from pET3c (43) by the removal of the *EcoRV* fragment.

To construct plasmid pAR8-10, the *ClaI* fragment of plasmid pAR8 (Fig. 1) was replaced by a *ClaI* fragment of plasmid pAR7-8-8.5-9-10, resulting in a plasmid containing the gp8 and gp10 genes, plus the gp8.5 and gp9 genes, which are not essential for procapsid assembly.

To construct plasmid pAR7-10, plasmid pAR7-8-8.5-9-10 was digested with *NheI* and then partially with *XbaI* to remove the gp8, gp8.5, and gp9 genes. The *NheI* and *XbaI* digestion produced compatible cohesive ends. Ligation of digested products produced plasmid pAR7-10 containing the gp7 and gp10 genes.

To construct plasmid pARd7-8-8.5-9-10, a DNA fragment containing only the gp7 gene was synthesized by PCR with primer pair 215D (Table 1) and M13 reverse primer, using plasmid pBlue6K (18) as a DNA template. Plasmid pBlue6K is a pBlueScript KS(+) derivative containing ϕ29 the gp7, gp8, gp8.5, gp9, and gp10 genes. Primer 215D targeted at the end of the gp7 coding sequence and contained a *NdeI* site to generate a new site for cloning. The resulting PCR fragment had *NdeI* restriction sites at both ends. After digestion with *NdeI*, the DNA fragment was inserted into the 5' *NdeI* site of plasmid pARgp7 (18) containing the gp7 gene, yielding plasmid pARd7 carrying duplicated gp7 genes fused from COOH to NH₃ termini without a stop codon. The *NheI*-*BamHI* fragment from plasmid pARgp7-8-8.5-9-10 was cloned into the *NheI*-*BamHI* sites of plasmid pARd7 to produce plasmid pARd7-8-8.5-9-10.

To construct plasmid pAR10, the *XbaI* fragment containing the gp7, gp8, gp8.5, and gp9 genes was deleted from plasmid pARgp7-8-8.5-9-10.

To construct plasmid pAR7-8-8.5-20, a DNA fragment containing phage T4

portal vertex gene 20 was generated by PCR using plasmid pR20-4-6, kindly provided by L. W. Black (35), as a template with primers GP20F and GP20R containing *BamHI* sites (Table 1). The PCR fragment was then digested with *BamHI* and inserted into the *BamHI* site of plasmid pAR7-8-8.5 (18). The resulting plasmid, pAR7-8-8.5-20, contained the genes coding for gp7, gp8, and gp8.5 of ϕ29 and gp20 of T4.

To construct plasmid pAR7M-8-8.5-10/*NdeI*, the *KpnI*-*ClaI* fragment from plasmid pBlue6K (18) was inserted into *KpnI*-*ClaI* sites of plasmid pBlueScriptSK(+), resulting in plasmid pBlue7. A DNA fragment was produced by PCR using plasmid pBlue7 as a template with primers GP7F and GP7QN (Table 1). GP7QN had three base mutations at the 3' end of the gp7 gene, causing the mutation of three acidic amino acids at the C-terminal region of gp7 to neutral ones (Fig. 1). This PCR DNA fragment was used as a megaprimer in the following PCR. The PCR DNA fragment containing mutant gp7 was synthesized by using plasmid pBlue7 as a template with the megaprimer and M13 reverse primer. This second PCR DNA fragment was digested with restriction enzymes *NdeI* and *NheI* and inserted between the *NdeI* and *NheI* sites of plasmid pAR7-8-8.5-10/*NdeI* (53). Plasmid pAR7M-8-8.5-10/*NdeI* is the same as plasmid pAR7-8-8.5-10/*NdeI* except for a three-base mutation in the gp7 gene.

To construct plasmids pAR7-7-8-8.5-9-10, pAR8-7-8-8.5-9-10, and pAR10-7-8-8.5-9-10, the *BglII*-*BamHI* fragments from plasmids pARgp7, pAR8, and pAR10, respectively, were inserted into the *BglII* site of plasmid pAR7-8-8.5-9-10 (18).

To construct plasmids pSK8 and pSK10, the *BglII*-*BamHI* fragments from plasmids pAR8 and pAR10, respectively, were inserted into the *BamHI* site of pBlueScriptSK(+).

To construct plasmid pAR8-7-10, the *XbaI* fragment from plasmid pSK8 was inserted into the *XbaI* site of plasmid pAR7-10.

To construct plasmid pAR10-7-8-8.5, the *XbaI* fragment from plasmid pSK10 was inserted into the *XbaI* site of plasmid pAR7-8-8.5.

Expression and purification of structural proteins. The purification of gp10 has been described elsewhere (25). However, the system used for protein overproduction in this study is different from the one reported by Ibanez et al. (25). The procedures described by Guo and Moss (20) and Guo et al. (18) were followed for induction and expression with the use of *E. coli* HMS174(DE3) or HMS174(DE3)/pLysS as the host.

To purify capsid protein gp8, a 1-liter bacterial culture was centrifuged after induction. The pellet was resuspended in 10 mM TMS buffer (0.05 M Tris-Cl [pH 7.8], 0.01 M MgCl₂, 0.1 M NaCl), lysed in a French pressure cell, and centrifuged at 2,000 × *g* for 10 min to remove cell debris. The supernatant containing gp8 was then centrifuged at 12,000 × *g* for 10 min. The pellets (containing inclusion bodies) were dissolved in 10 ml of GncI buffer (0.01 M Tris-Cl [pH 7.5], 0.005 M dithiothreitol, 6 M guanidinium chloride) and centrifuged at 100,000 × *g* for 1 h. The supernatant was dialyzed against TMS buffer overnight at room temperature.

To analyze the formation of procapsid by sucrose gradient, a 100-ml bacterial culture was induced with isopropylthiogalactopyranoside (IPTG), collected by centrifugation, and resuspended in 0.5 ml of MMS buffer (2 mM sodium azide, 5 mM maleic acid [pH 5.6], 0.1 M NaCl, 15 mM MgCl₂). The cells were broken by sonication and sedimented at 10,000 rpm for 10 min to remove cell debris. The supernatant was loaded onto a 5 to 20% sucrose gradient in MMS buffer and centrifuged at 35,000 rpm for 30 min at 20°C with an SW55 rotor. The opaque bands, which contained particles, were isolated and examined by electron microscopy.

Biological assay for phage assembly after *E. coli* extract complementation. The synthesis and purification of pRNA (48, 52–54), gp16 (19), and DNA-gp3 (32), as well as the preparation of extracts (32), have been reported. The two *E. coli* extracts (10 ml), containing one or two ϕ29 procapsid structural proteins, were mixed and incubated for 2 h at ambient temperature to assay procapsid formation by complementation. In vitro ϕ29 assembly was performed as previously described (32, 33), using the complementation mixtures described above as sources of procapsids.

Assay for efficiency of procapsid formation by sucrose gradient sedimentation. One-milliliter overnight cultures of *E. coli* HMS174(DE3) containing plasmid pARgp7-8-8.5-9-10, pARgp7-8-8.5-10/*NdeI*, pAR7-7-8-8.5-9-10, pAR8-7-8-8.5-9-10, pAR10-7-8-8.5-9-10, pAR8-7-10, or pAR10-7-8-8.5 were diluted in 100 ml of Superbroth (20) containing 50 μg of ampicillin per ml. After incubation for 2 h at 37°C, IPTG was added to a final concentration of 0.5 mM, and the mixtures were incubated for an additional 2 h. The bacteria were harvested by centrifugation, and cell pellets were suspended in 10 ml of buffer A (20). The cells were then lysed by passage through a French press cell. Cell debris was removed by centrifugation at 12,000 × *g* for 30 min. The supernatants were loaded on 10 to 30% (wt/vol) sucrose gradient in MMS buffer and centrifuged at 25,000 rpm for 4.5 h with an SW28 rotor. The procapsid bands were identified under visible light.

Electron microscopy. Micrographs with negative staining were prepared by John Turek. Samples were spotted on 400-mesh grids covered with Formvar-carbon. The grids were washed three times with distilled water and negatively stained with 1.5% aqueous uranyl acetate solution. After drying on filter paper, the sample grids were examined with a JEOL 100CX electron microscope. The micrographs of cryoelectron microscopy were prepared by Tim Baker and Norman Olson as described previously (18).

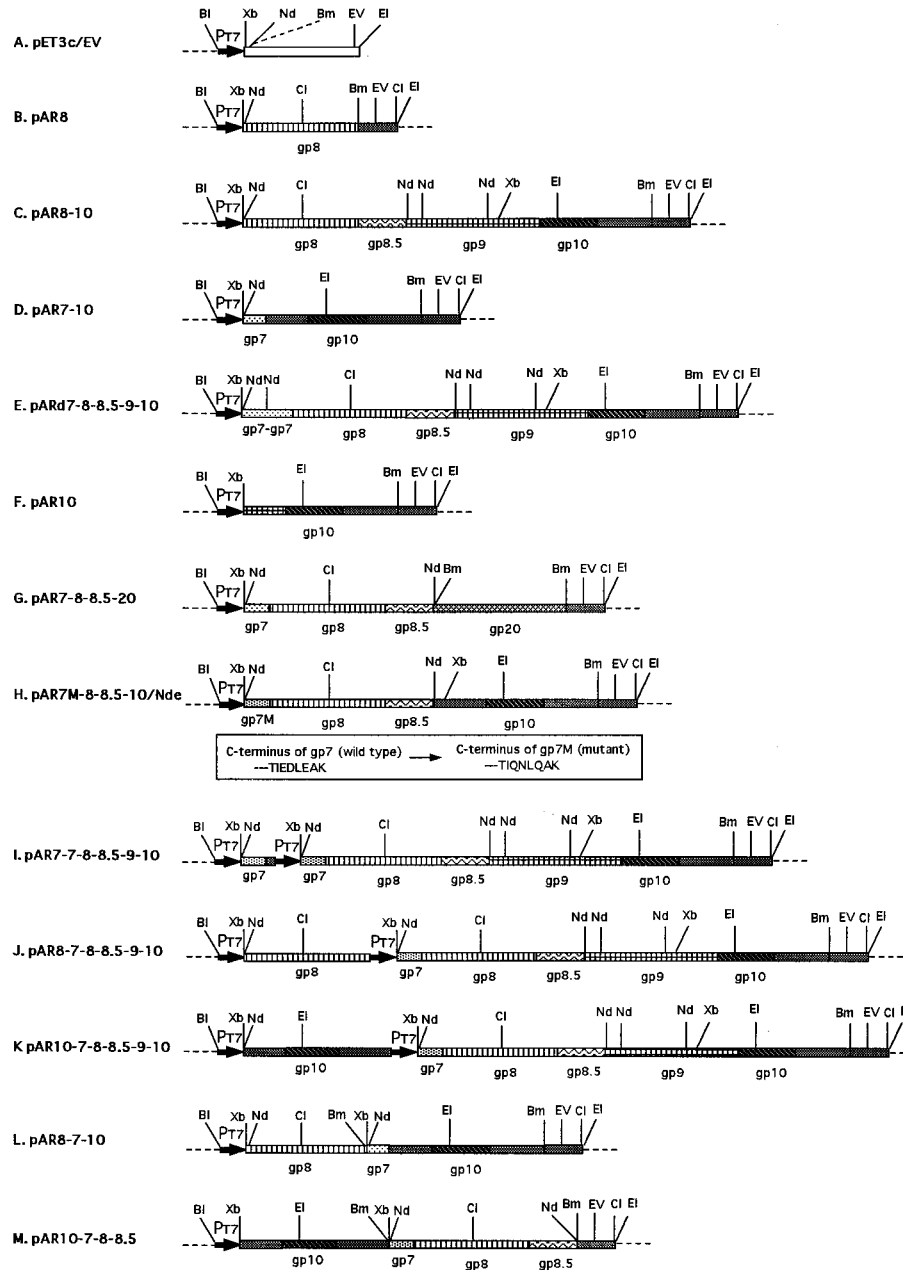


FIG. 1. Outline of plasmid construction showing the polylinker sites, gene inserts, and certain relevant restriction sites. P_{T7}, T7 promoter; Bl, *Bgl*II; Bm, *Bam*HI; Cl, *Cl*I; Ei, *Eco*RI; EV, *Eco*RV; Nd, *Nde*I; Xb, *Xba*I.

RESULTS

Comparison of the solubilities and structure formation of the scaffolding (gp7), capsid (gp8), and portal vertex (gp10) proteins expressed alone in *E. coli*. To study the sequential interaction among the structural components, it is essential to investigate the solubility and structure formation of each component when expressed alone. The solubility of gp7 (18) and the formation of portal vertex particles (5) have been reported. However, it is necessary to compare the three structural components with identical overproduction systems.

E. coli HMS174(DE3)/pLysS cells, harboring plasmid pARgp7 (18), were induced with IPTG to overproduce the scaffolding protein. When these cells were lysed and centri-

TABLE 1. Primers used for PCR

Name	Sequence
GP8F	5'-TACAACACATATGCGAA-3' <i>Nde</i> I
GP8R	5'-AGTAAATGGATCCATCA-3' <i>Bam</i> HI
215D	5'-TTACATATGCTTTGCTTCT-3' <i>Nde</i> I
GP20F	5'-ATGGATCCCATTGAG-3' <i>Bam</i> HI
GP20R	5'-AAAGGATCCATTA-3' <i>Bam</i> HI
GP7F	5'-AAGAGGTGAAACATATG-3' <i>Nde</i> I
GP7QN	5'-TGCTTGTAAGTTCTGGAT-3'

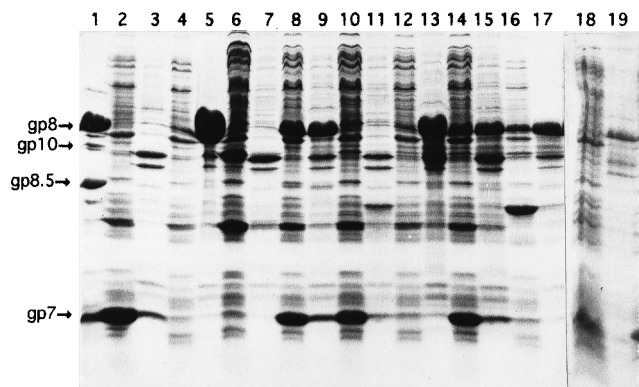


FIG. 2. SDS-PAGE for the analysis of the solubility of ϕ 29 procapsid structural proteins. After induction, *E. coli* cells (3 ml) were centrifuged and resuspended in 0.5 ml of buffer A. After freeze-thawing, the lysates were centrifuged at $1,000 \times g$ for 10 min to remove the cell debris. The supernatant was centrifuged again at $16,000 \times g$ for 30 min. The pellets were dissolved in 0.2 ml of buffer A and subjected to SDS-PAGE side by side with the corresponding supernatants. Lane 1, purified ϕ 29 procapsid. Even-numbered lanes contained supernatants and odd-numbered lanes contained pellets of *E. coli* harboring the following plasmids: lane 2 and 3, pARgp7; lane 4 and 5, pAR8; lane 6 and 7, pAR10; lane 8 and 9, pAR7-8-8.5; lanes 10 and 11, pAR7-10; lanes 12 and 13, pAR8-10; lanes 14 and 15, pAR7-8-8.5-9-10; lanes 16 and 17, pARd7-8-8.5-9-10; and lanes 18 and 19, pAR7M-8-8.5-10/Nde.

fused, the majority of the scaffolding protein was in the supernatant (Fig. 2, lanes 2 and 3). After purification, gp7 was applied to a 5 to 20% sucrose gradient and centrifuged at 35,000 rpm for 30 min; subsequently, each fraction of this gradient was analyzed by sodium dodecyl sulfate-polyacrylamide gel electrophoresis (SDS-PAGE). The scaffolding proteins stayed on top of the gradient, indicating that these proteins did not aggregate to form particles and supporting our previous report that the purified scaffolding protein existed in a soluble form (18). In contrast, in phage T4 (46, 47) and herpes simplex virus, the scaffolding protein alone forms particles (39). The purified gp7 monomers were measured by circular dichroism with a Jasco J600 spectropolarimeter. When predicted from the circular dichroism spectrum by the method of Yang et al. (51), the secondary structure of gp7 was mostly composed of α helices (data not shown), a result in accord with the report that

a high ratio of α helices is found in the scaffolding protein of phage T4 (34).

When the portal vertex proteins were expressed in *E. coli* HMS174(DE3)/pLysS harboring plasmid pAR10, these proteins assembled into connectors that automatically formed a tetragonal array when observed by electron microscopy with negative staining (Fig. 3A). They were also present in the supernatant (Fig. 2, lanes 6 and 7).

When the capsid protein gp8 was expressed in *E. coli* HMS174(DE3)/pLysS harboring plasmid pAR8, most capsid proteins aggregated in the cells to form inclusion bodies, and the majority precipitated when centrifuged after cell lysis (Fig. 2, lanes 4 and 5). The precipitated capsid proteins were isolated and denatured in 6 M guanidinium chloride and renatured in TMS buffer. When the renatured product was examined by electron microscopy, only aberrant structures were found. Some capsid proteins in *E. coli* were in the supernatant after centrifugation, and these proteins also formed aberrant structures (Fig. 3B), indicating that the behavior of the capsid protein of this double-stranded DNA virus is different from the capsid protein of RNA viruses, of which the capsid proteins assemble into virus-like particles when expressed alone (12, 13, 26).

Formation of gp7-gp8 particles and unstable gp7-gp10 complexes. When the genes coding for scaffolding protein gp7 and capsid protein gp8 were coexpressed in *E. coli* harboring plasmid pARgp7-8-8.5, the majority of the proteins stayed in the supernatant when the cell lysate was subjected to centrifugation (Fig. 2, lanes 8 and 9). These capsid proteins formed procapsid-like structures of various sizes and shapes (18). These results indicated that in the absence of gp7, gp8 did not have the capability to assemble into procapsid, and gp7 prevented the capsid proteins from forming inclusion bodies.

When gp7 and gp10 were coexpressed in *E. coli* harboring plasmid pAR7-10, both proteins remained in the supernatant (Fig. 2, lane 10 and 11). The complex of gp7 and gp10 was identified by sucrose gradient sedimentation (data not shown; a result similar to that shown in Fig. 4 [see below]). However, the majority of gp7 and gp10 remained separated, indicating that the complex was unstable.

gp7 and gp10 were purified, mixed, and dialyzed successively against TBE and TMS buffers for 20 min each at ambient temperature. The mixture was applied to a 5 to 20% sucrose

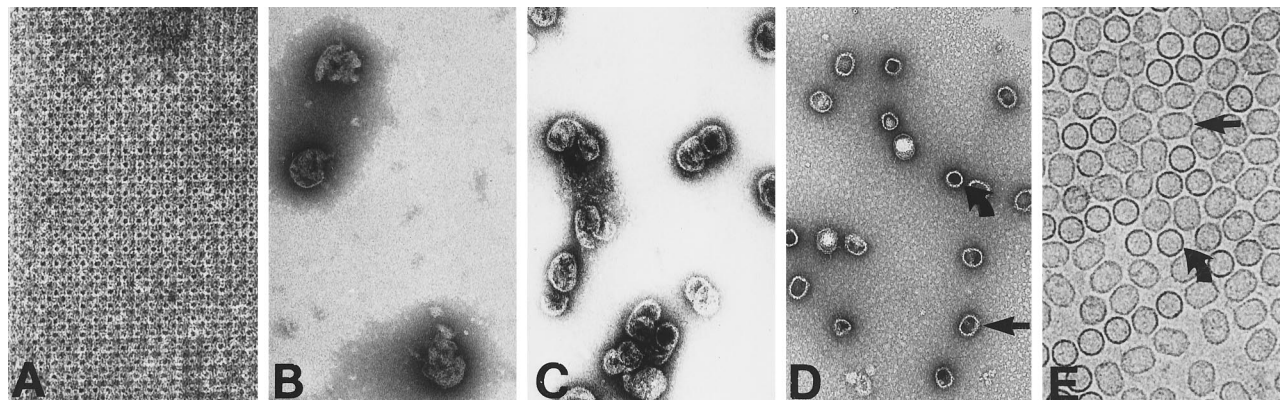


FIG. 3. Negatively stained (A to D) and cryoelectron (E) micrographs of ϕ 29 structural components. (A) Purified portal vertex; (B) particles from *E. coli* containing plasmid pAR8; (C) particles from *E. coli* containing plasmid pARd7-8-8.5-9-10; (D and E) procapsids from *E. coli* containing plasmid pAR7-8-8.5-9-10. In panels B and C, *E. coli* cells were lysed by sonication and centrifuged. The supernatants were examined by electron microscopy directly. The linear arrows in panels D and E show the typical prolate shape of ϕ 29 procapsid, and the curved arrows indicate the procapsids oriented with their long axes perpendicular to the plane of view. Magnifications: (A) $\times 125,000$; (B and C) $\times 82,500$; (D) $\times 25,000$; (E) $\times 100,000$.

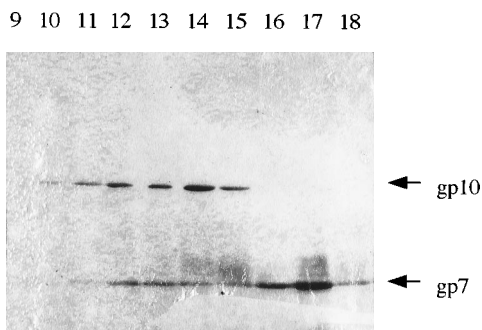


FIG. 4. SDS-PAGE of fractions from sucrose gradients showing the interaction of scaffolding (gp7) and portal vertex (gp10) proteins. The purified gp7 and gp10 were mixed and dialyzed against TBE and TMS for 20 min each at room temperature. The mixture was applied to 5 to 20% sucrose gradient and centrifuged at 35,000 rpm with a Beckman SW55 rotor for 2 h. Sedimentation was from right to left; fraction numbers are indicated.

gradient in TMS and centrifuged for 2 h at 35,000 rpm, using a Beckman SW55 rotor. The gradient fractions were analyzed by SDS-PAGE (Fig. 4). The particle with the faster sedimentation rate appeared at fraction 12, which contained both gp10 and gp7. A peak at fraction 14 represents portal vertex itself without the binding of gp7. Without the portal vertex proteins, the scaffolding proteins stayed on the top of the gradient (data not shown). Formation of a gp7-gp10 complex has also been demonstrated by mixing a fixed concentration of gp10 with increasing amounts of gp7 to observe an increase in the migration rate of the product in a nondenaturing agarose gel (18). However, the scaffold-portal vertex complexes did not form procapsid-like particles, since more scaffolding proteins (about 111 copies per one procapsid) should have interacted with the portal vertex proteins (12 to 13 copies per one procapsid) to form procapsid-like particles. Only a small portion of the scaffolding proteins interacted with portal vertex proteins, indicating that the gp7-gp10 particles were unstable in the absence of capsid protein gp8.

Cloning and coexpression of genes coding for gp8 and gp10.

The genes coding for the capsid protein gp8 and the portal vertex protein gp10 were cloned and coexpressed in *E. coli* harboring plasmid pAR8-10. When the cell lysate was subjected to centrifugation, the capsid proteins were found in precipitated fractions as observed when the capsid protein was expressed alone (Fig. 2, lanes 12 and 13). The portal vertex proteins were in the supernatant fraction, similar to the expression of portal vertex alone. The result demonstrated that the two proteins did not interact. Capsid proteins in the supernatant fraction formed aberrant structures which were the same as those from the *E. coli* harboring plasmid pAR8 (Fig. 3B).

Complementation of *E. coli* extracts containing one or two procapsid structural proteins. One approach to determine the pathways in procapsid assembly is to isolate the procapsid assembly intermediates and/or to convert the intermediates to infectious mature virions. Both the gp7-gp8 and gp7-gp10 complexes are possible candidates. The most reliable way to answer this question is to determine whether the complexes themselves can be converted to infectious virions.

E. coli extracts containing gp7-gp8 complexes were complemented with an extract containing protein gp10 and assayed for biological activity by the in vitro ϕ 29 assembly system. This system provided the ϕ 29 DNA-gp3, pRNA, DNA-packaging protein gp16, ATP, and neck and tail proteins. If the procapsids were assembled from gp7-gp8 complexes plus protein

TABLE 2. In vitro complementation to analyze procapsid formation with in vitro ϕ 29 assembly system

Expt	Complementation of extracts ^a	PFU/ml ^b (10^5)
1	gp7-8 + gp10	0
2	gp8-10 + gp7	0
3	gp7-10 + gp8	0
4	gp7 + gp8 + gp10	0
5	gp7-8 + gp8-10 + gp7-10	0
6	gp7-8-8.5-10/Nde	5.0

^a *E. coli* extracts containing one or two structural proteins were complemented by incubation for 2 h at ambient temperature and then used as procapsid sources for in vitro ϕ 29 assembly.

^b Average of three experiments.

gp10, active procapsids would package DNA-gp3, and the DNA-filled capsids would be converted to infectious phages by the assembly of necks and tails as reported previously (32, 33). No plaques were produced by complementation of gp7-gp8 complexes with gp10 (Table 2, experiment 1). Zero dilution also gave no plaques, even when all of the packaging mixtures were plated. The gp7-gp8 particles were isolated from the lysate of *E. coli* containing plasmid pARgp7-8-8.5 by sucrose gradient sedimentation to remove the noninteracted individual gp7 and gp8 proteins. The complementation of purified gp7-gp8 complexes with purified protein gp10 also produced no procapsids when assayed with the sensitive in vitro ϕ 29 assembly system.

Similar results were obtained when *E. coli* extracts containing gp8-gp10 or gp7-gp10 complexes were complemented with extracts containing gp7 or gp8, respectively (Table 2, experiments 2 and 3). No plaques were identified after complementation of the three *E. coli* extracts containing gp7, gp8, and gp10 (Table 2, experiment 4).

The concatemeric gp7 dimer promoted the solubility of gp8 but was inactive in procapsid assembly. The gp7 gene lacking a stop codon was inserted upstream of another gp7 gene in plasmid pARgp7-8-8.5-10 to produce a head-to-tail dimer of the scaffolding protein. Proteins with molecular weights twice that of the normal gp7 could be detected by SDS-PAGE (Fig. 2, lane 16). Only aberrant structures with a low degree of organization were found, similar to those found in cells expressing the gp8 gene alone (Fig. 3C). However, capsid proteins were found in the supernatant when dimeric gp7 was coexpressed (Fig. 2, lanes 16 and 17), indicating that the dimeric fusion scaffolding protein could interact with the capsid proteins and prevent them from forming inclusion bodies. However, the fusion proteins were inactive in the assembly of normal procapsids, possibly because of incorrect folding.

Inactivation of the scaffolding protein by mutation of three amino acids in the C-terminal region. The three acidic amino acids, Glu and/or Asp, within the final eight-amino-acid stretch of gp7 were mutated to neutral amino acids, Gln and Asn (Fig. 1). When the mutant gp7 was coexpressed with wild-type gp8 and gp10 in *E. coli* containing plasmid pAR7M-8-8.5-10/Nde, gp8 formed inclusion bodies (Fig. 2, lanes 18 and 19). The mutant scaffolding proteins lost the ability to interact with capsid proteins and could not prevent gp8 from forming inclusion bodies.

Coexpression of portal vertex protein gp20 of T4 with ϕ 29 scaffolding and capsid proteins. It was reported that the portal protein gp10 of ϕ 29 could be incorporated into the procapsid of phage lambda (8). To investigate whether chimeric ϕ 29-T4 procapsids can be constructed, the gene coding for the portal protein gp20 of T4 was inserted into plasmid pARgp7-8-8.5 to

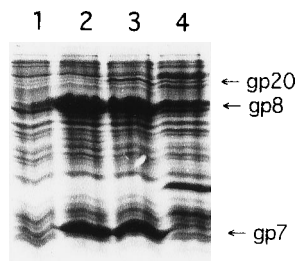


FIG. 5. SDS-PAGE (15% polyacrylamide gel) showing the coexpression of T4 portal protein gp20 with φ29 scaffolding protein gp7 and capsid protein gp8 in *E. coli* with the following plasmids: lane 1, pET3c/EV; lane 2, pAR7-8-8.5; lane 3, pAR7-8-8.5-20; and lane 4, pR20-4-6.

generate plasmid pAR7-8-8.5-20. The gp20 of T4 was coexpressed with the scaffolding protein gp7 and capsid protein gp8 of φ29 (Fig. 5). The lysate of *E. coli* harboring plasmid pAR7-8-8.5-20 was fractionated by sucrose gradient sedimentation. Particles with variable shapes and sizes were observed under electron microscopy, a result similar to that for the lysate of *E. coli* harboring the plasmid containing the genes encoding gp7 and gp8 only (18), indicating the lack of interaction between the T4 portal protein and φ29 scaffolding and capsid proteins.

Unbalanced overproduction of one of the structural components. To test whether perturbing the ratio of the three structural components of the φ29 procapsid could affect its assembly, one of the structural genes was duplicated by insertion of the gene into the coexpression plasmid pAR7-8-8.5-9-10 (Fig. 1). The resulting plasmids, pAR7-7-8-8.5-9-10, pAR8-7-8-8.5-9-10, and pAR10-7-8-8.5-9-10, were used to perturb the ratio of scaffolding, capsid, and portal vertex proteins, respectively, in *E. coli* (Fig. 1). The efficiency of procapsid formation was assayed by sucrose gradient sedimentation and by plaque formation analysis with the highly sensitive φ29 assembly system (32). Results from both sucrose gradient and sensitive system analyses showed that no difference could be demonstrated with lysates of *E. coli* harboring plasmids pAR7-7-8-8.5-9-10, pAR8-7-8-8.5-9-10, and pAR10-7-8-8.5-9-10 compared with a lysate of *E. coli* harboring the normal coexpression plasmid pAR7-8-8.5-9-10 (Table 3).

Changing of the order of gene arrangement in plasmids coexpressing the structural proteins. To investigate the effect of changing the order of gene arrangement on procapsid formation, the positions of genes coding for gp7, gp8, and gp10 were switched in the coexpression plasmids (Fig. 1). For example, in plasmid pAR10-7-8-8.5, the portal vertex gp10 gene

TABLE 3. Effect of unbalanced overproduction of one procapsid structural protein on procapsid formation^a

Plasmid (gene arrangement) ^b	Avg PFU/ml ± SD (10 ⁴) ^c
pAR7-7-8-8.5-9-10 (P-SD-7-P-SD-7-SD8-SD-8.5-SD-9-SD-10).....	0.79 ± 0.42
pAR8-7-8-8.5-9-10 (P-SD-8-P-SD-7-SD8-SD-8.5-SD-9-SD-10).....	0.49 ± 0.19
pAR10-7-8-8.5-9-10 (P-SD-10-P-SD-7-SD8-SD-8.5-SD-9-SD-10).....	0.28 ± 0.18
pAR7-8-8.5-9-10 (P-SD-7-SD8-SD-8.5-SD-9-SD-10).....	0.37 ± 0.28

^a Extracts of *E. coli* harboring the individual plasmids were used as procapsid sources for in vitro φ29 assembly.

^b P and SD denote T7 promoter and Shine-Dalgarno sequence, respectively.

^c Average of three experiments.

TABLE 4. Effect of the order of gene arrangement on procapsid formation^a

Plasmid (gene order)	Avg PFU/ml ± SD (10 ⁴)	No. of expts
pAR10-7-8-8.5 (P-SD-10-SD-7-SD-8-SD-8.5)	2.39 ± 2.39	6
pAR8-7-10 (P-SD-8-SD-7-SD-10)	0.53 ± 0.26	5
pAR7-8-8.5-10/Nde (P-SD-7-SD-8-SD-8.5-SD-10)	0.96 ± 0.53	6

^a For details, see the footnotes to Table 3.

was positioned in front of the genes for gp7 and gp8 (Fig. 1). All of the three genes were driven by a single T7 promoter to produce a single polycistronic mRNA. Each gene contained its own Shine-Dalgarno sequence for ribosome binding. The efficiency of procapsid formation was assayed by sucrose gradient sedimentation and by plaque formation analysis with the in vitro φ29 assembly system (32). Results from both sucrose gradient and assembly system analyses indicated that no differences could be demonstrated with lysates of *E. coli* harboring the plasmids with the gene order 8 → 7 → 10 or 10 → 7 → 8 compared with the lysate of *E. coli* harboring the coexpression plasmid pAR7-8-8.5-9-10, in which the gene order was identical to that in the φ29 genome (Table 4).

DISCUSSION

If φ29 procapsid assembly follows the single-assembly pathway, the sequential interaction in φ29 procapsid assembly should be one of the following three possibilities: (i) scaffolding proteins + capsid proteins → scaffolding-capsid complex + portal vertex proteins → procapsid; (ii) capsid proteins + portal vertex proteins → capsid-portal vertex complex + scaffolding proteins → procapsid; or (iii) scaffolding proteins + portal vertex proteins → scaffolding-portal vertex complex + capsid proteins → procapsid. It was found that if only the scaffolding and capsid proteins were coexpressed in *E. coli*, they formed particles which varied in size and shape (18). Therefore, the first pathway might not be correct because the size and shape of normal procapsids should have been diverse if portal vertex proteins were inserted into these preformed scaffolding-capsid particles. The portal vertex protein, therefore, is not the final component added to the scaffolding-capsid protein complex during procapsid assembly. Our results also exclude the possibility of the second pathway because capsid and portal vertex proteins did not interact with each other. Also, our results would not agree with the third pathway because if that pathway were correct, the gp7-gp8 particles could not be formed. No procapsids were produced when *E. coli* extracts containing one or two structural components of procapsids were complemented (Table 2). When gp7, gp8, and gp10 were coexpressed in *E. coli*, active procapsids (18, 21) that could be converted into infectious virions after DNA packaging and neck and tail assembly (32, 33) were formed. These results indicate that the true procapsid assembly intermediates composed of only two structural components are unstable or cannot be formed, or they could not be used in vitro because of the possible involvement of host components, such as chaperone GroE. The three components, i.e., scaffolding, capsid, and portal vertex proteins, must coexist for assembly to occur. In an equilibrium model, Zlotnick (55) proposed that the extent of viral assembly at equilibrium is extremely concentration dependent and highly cooperative. He deduced a sigmoidal curve describing a

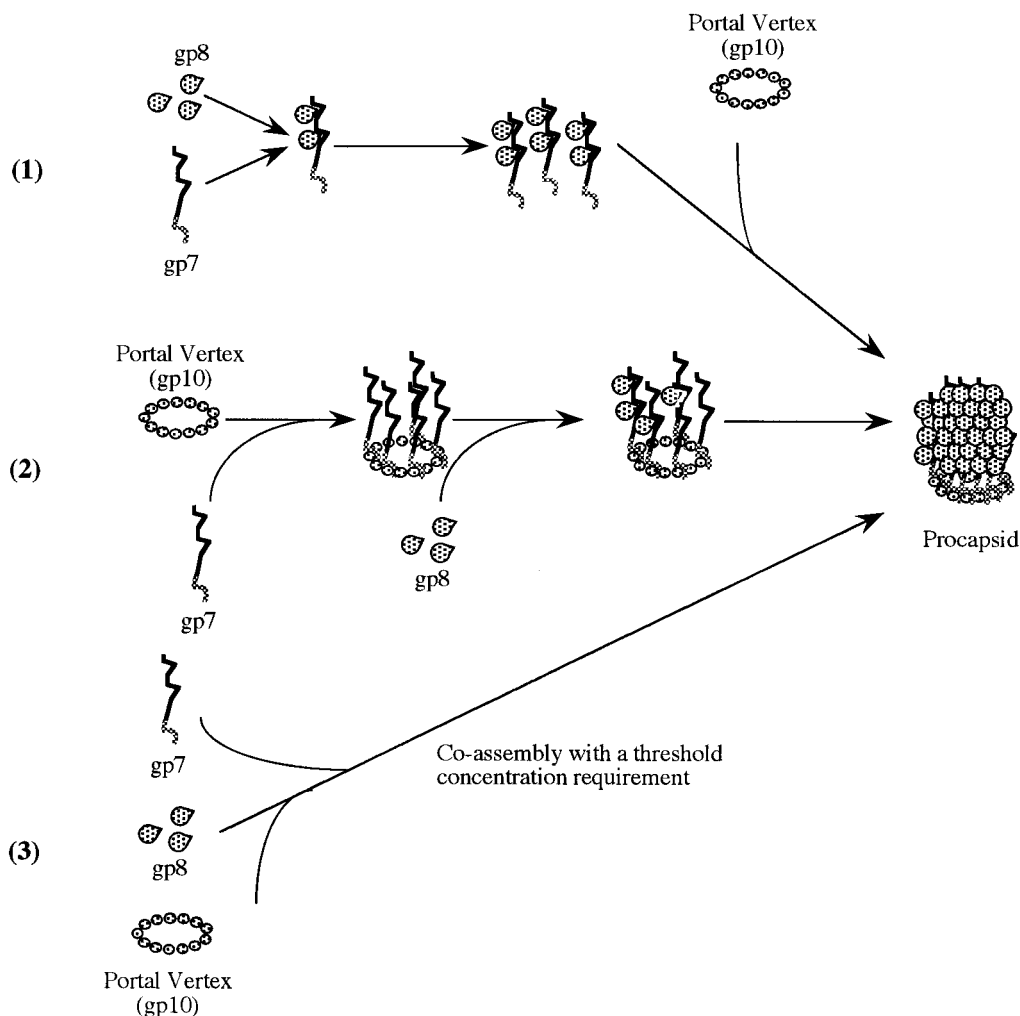


FIG. 6. Three models of $\phi 29$ procapsid assembly (see Discussion for details). In model 1, the scaffolding protein gp7 and capsid protein gp8 interact first, forming heterodimers or hetero-oligomers. The gp7-gp8 complexes then interact with the portal vertex consisting of 12 or 13 copies of gp10 to form active procapsids. In model 2, the portal vertex serves as an initiator to interact with gp7, which bridges gp8 and gp10. The number of gp7 molecules recruited by gp10 could subsequently determine the number of gp8 molecules incorporated into the matured procapsid. Therefore, both gp10 and gp7 play roles in the determination of procapsid shape and size. In model 3, there are trimolecular interactions of gp7, gp8, and gp10 with a threshold concentration requirement. gp7 also serves as a bridge for gp10 and gp8, and both gp7 and gp10 play roles in procapsid shape and size determination as in model 2.

12th-power concentration dependence for assembly of a dodecahedral capsid, using the equation

$$[v] = 5^{11} \frac{1}{12} e^{-30\Delta G_c/RT} [s]^{12}$$

where $[v]$ and $[s]$ are concentrations of assembled capsids and free capsid subunits, respectively, ΔG_c is free energy of subunit association (-4.08 kcal [1 cal = 4.184 J]/mol), R is the gas constant (1.987 cal degree $^{-1}$ mol $^{-1}$), and T is temperature (298 K). Although this model is deduced from analyzing the assembly of a model procapsid composed of only one species of protein, by analogy it could apply to $\phi 29$ procapsid assembly as well. The procapsid of $\phi 29$ could not assemble until the concentration of each of the three structural components reached a certain value (threshold concentration requirement). As soon as the threshold concentration requirement was fulfilled, cointeraction of the three components occurred so rapidly that stable intermediates could not be isolated. This rapid assembly prevented aberrant structures from accumulat-

ing. With his equilibrium model, Zlotnick (55) also predicted that intermediates existed for very short periods of time in viral capsid assembly. Assembly intermediates or intermediate particles have been identified in other double-stranded DNA viruses or phages (39, 40, 46, 47). Whether these are really identical to the active intermediates that appear during the procapsid assembly process remains to be proven by experiments to convert these intermediates into infectious viral particles.

For most bacteriophage genes, their positions in the genome reflect the interactions between their products (7). For example, the gpD and gpE proteins of bacteriophage λ interact, and these genes are adjacent (6, 50). Also, the N and C termini of λ gpA protein interact with gpNu1 protein and procapsid, respectively. Thus, the A gene lies between Nu1 and genes coding for the structural proteins of λ procapsid (10, 11). The genes encoding the scaffolding proteins of all known bacteriophages are positioned in front of capsid genes (7). To test if the gene positions have any significant meaning, the positions of

three procapsid structural genes were changed. Interestingly, no differences in procapsid formation were found when the positions of procapsid structural genes were changed (Table 4). This result indicates that the gene positions do not always reflect the interactions of gene products and also favors the model of trimolecular interactions with a threshold concentration requirement.

Beyond the single-assembly pathway, there are still three possible models for procapsid assembly (Fig. 6). In the first model, the scaffolding and capsid proteins interact first to form heterodimers or hetero-oligomers (probably pentamers or hexamers), which then interact with the portal vertex to form an initiation complex. After initiation, more scaffolding-capsid complexes are assembled into the initiation complex to finish the procapsid. The problem with this pathway is how to prevent the formation of the portal vertex-lacking scaffold-capsid particles with variable shapes and sizes as reported previously (18). In the second model, the scaffolding and portal vertex proteins interact first, and the capsid proteins are subsequently added to the scaffold-portal vertex initiation complex. However, the ϕ 29 scaffold-portal vertex complexes were unstable. Also, the other problem of this pathway is how to prevent the formation of the aberrant scaffold-capsid particles. One possibility is that the presence of portal protein could make correct assembly more rapid, thus kinetically blocking the formation of the aberrant scaffold-capsid complexes, which might form more slowly. This possibility suggests that the gp7-gp10 complexes can be complemented by the addition of gp8. However, our results do not support this speculation (Table 2, experiment 3). The failure of gp8 to complement an extract containing gp7-gp10 complexes is possibly due to the aggregation of the gp8 within the overproducing cells. In the third model, a trimolecular interaction among scaffolding, capsid, and portal vertex proteins with a threshold concentration is required to assemble a functional ϕ 29 procapsid. As discussed above, our data do not support the first or the second model but favor the third one. Interpretation of data from the *in vitro* study is complicated by the fact that host factors are known to participate in ϕ 29 procapsid assembly (41) and might participate in the triple interaction. Our argument against binary assembly followed by the addition of a third component remains to be further verified by more *in vivo* studies. Interaction of gp7 with gp8 has been documented by the finding that particles with variable shapes and sizes were assembled when gp7 and gp8 were coexpressed (18). Interaction of gp7 with gp10 was observed when gp7 and gp10 were mixed or coexpressed. In all models, gp7 molecules are speculated to serve as bridges to link, and contain two domains to bind, gp10 and gp8, respectively. This speculation is also supported by findings described below. When the capsid protein and the portal protein were coexpressed, the capsid proteins were still present in the insoluble fraction and did not interact with portal proteins. This means that the portal proteins did not prevent the aggregation of capsid proteins and the scaffolding proteins were required to do so. Though not able to participate in procapsid assembly, dimeric gp7 could, while gp7 with a C-terminal region mutation could not, prevent the capsid proteins from forming inclusion bodies. Therefore, the C terminus of gp7 might be important for scaffolding-capsid protein interaction. The scaffolding protein of phage P22 contains at least two folding domains. The ϕ 29 scaffolding protein could possess a similar property. One domain, probably the C terminus, interacts with capsid protein to keep it from forming an inclusion body, and the other participates in the interaction with the portal vertex. A definite number of gp7 molecules recruited by the gp10 oligomer (portal vertex) would concomitantly determine the

number of gp8 molecules to be incorporated into the procapsid. Therefore, both gp7 and gp10 play key roles in procapsid shape and size determination. This interpretation explains why gp7-gp8 procapsid-like particles with variable shapes and sizes have been produced in the absence of the portal protein gp10 (18).

ACKNOWLEDGMENTS

We thank T. S. Baker, N. Olson, J. Turek, and D. Van Horn for electron micrographs; L. Black for plasmid pR20-4-6; S. Erickson for the preparation of Fig. 4; and K. Ostanin and R. L. Van Etten for circular dichroism spectrum analysis of gp7.

This work was supported by NIH grants GM46490 and GM48159 to P.G.

REFERENCES

- Anderson, D. L., and B. Reilly. 1993. Morphogenesis of bacteriophage ϕ 29, p. 859-867. In A. L. Sonenshein, J. A. Hoch, and R. Losick (ed.), *Bacillus subtilis* and other gram-positive bacteria: biochemistry, physiology, and molecular genetics. American Society for Microbiology, Washington, D.C.
- Bazinnet, C., and J. King. 1985. The DNA translocation vertex of dsDNA bacteriophages. *Annu. Rev. Microbiol.* **39**:109-129.
- Bazinnet, C., and J. King. 1988. Initiation of p22 procapsid assembly *in vivo*. *J. Mol. Biol.* **202**:77-86.
- Black, L. W. 1989. DNA packaging in dsDNA bacteriophages. *Annu. Rev. Microbiol.* **43**:267-292.
- Carazo, J. M., L. E. Donate, L. Herranz, J. P. Secilla, and J. L. Carrascosa. 1986. Three-dimensional reconstruction of the connector of bacteriophage ϕ 29 at 1.8 nm resolution. *J. Mol. Biol.* **192**:853-867.
- Casjens, S., and R. Hendrix. 1974. Locations and amounts of the major structural proteins in bacteriophage lambda. *J. Mol. Biol.* **88**:535-545.
- Casjens, S., and R. Hendrix. 1988. Control mechanisms in dsDNA bacteriophage assembly, p. 15-92. In R. Calendar (ed.), *The bacteriophages*, vol. 1. Plenum Publishing Corp., New York.
- Donate, L. E., and J. L. Carrascosa. 1991. Characterization of a versatile *in vitro* DNA packaging system based on hybrid λ/ϕ 29 proheads. *Virology* **182**:534-544.
- Duda, R. L., J. S. Wall, J. F. Hainfeld, R. M. Sweet, and F. A. Eiserling. 1985. Mass distribution of a probable tail-length-determining protein in bacteriophage T4. *Proc. Natl. Acad. Sci. USA* **82**:5550-5554.
- Earnshaw, W. C., and S. R. Casjens. 1980. DNA packaging by the double-stranded DNA bacteriophages. *Cell* **21**:319-331.
- Feiss, M. 1986. Terminase and the recognition, cutting and packaging of λ chromosomes. *Trends Genet* **2**:100-104.
- Frackman, S., D. A. Siegle, and M. Feiss. 1985. The terminase of bacteriophage λ : functional domains for *cosB* binding and multimer assembly. *J. Mol. Biol.* **180**:283-300.
- French, T. F., and P. Roy. 1990. Synthesis of bluetongue virus (BTV) corelike particles by a recombinant baculovirus expressing the two major structural core proteins of BTV. *J. Virol.* **64**:1530-1536.
- Gheysen, H. P., E. Jacobs, F. de Foresta, C. Thiriart, M. Francotte, D. Thines, and M. De Wilde. 1989. Assembly and release of HIV-1 precursor Pr55^{gag} virus-like particles from recombinant baculovirus-infected insect cells. *Cell* **59**:103-112.
- Guo, P. 1994. Introduction: principles, perspectives, and potential applications in viral assembly. *Semin. Virol.* **5**:1-3.
- Guo, P., S. Goebel, M. Perkus, J. Taylor, E. Norton, G. Allen, B. Languet, P. Desmettre, and E. Paoletti. 1990. Coexpression by vaccinia virus recombinants of equine herpesvirus 1 glycoproteins gp13 and gp14 results in potentiated immunity. *J. Virol.* **64**:2399-2406.
- Guo, P., E. Scholz, B. Maloney, and E. Welniak. 1994. Construction of recombinant avian infectious laryngotracheitis virus expressing the β -galactosidase gene and DNA sequencing of the insertion region. *Virology* **202**:771-781.
- Guo, P., E. Scholz, J. Turek, R. Nordgren, and B. Maloney. 1993. Assembly of avian infectious laryngotracheitis virus. *Am. J. Vet. Res.* **54**:2031-2039.
- Guo, P., S. Bailey, J. W. Bodley, and D. Anderson. 1987. Characterization of the small RNA of the bacteriophage ϕ 29 DNA packaging machine. *Nucleic Acids Res.* **15**:7081-7090.
- Guo, P., S. Erickson, and D. Anderson. 1987. A small viral RNA is required for *in vitro* packaging of bacteriophage ϕ 29 DNA. *Science* **236**:690-694.
- Guo, P., S. Erickson, W. Xu, N. Olson, T. S. Baker, and D. Anderson. 1991. Regulation of the phage ϕ 29 prohead shape and size by the portal vertex. *Virology* **183**:366-373.
- Guo, P., S. Grimes, and D. Anderson. 1986. A defined system for *in vitro* packaging of DNA-gp3 of the *Bacillus subtilis* bacteriophage ϕ 29. *Proc. Natl. Acad. Sci. USA* **83**:3505-3509.
- Guo, P., and B. Moss. 1990. Interaction and mutual stabilization of the two

- subunits of vaccinia virus mRNA capping enzyme co-expressed in *Escherichia coli*. Proc. Natl. Acad. Sci. USA **87**:4023–4027.
21. Guo, P., B. Rajagopal, D. Anderson, S. Erickson, and C.-S. Lee. 1991. sRNA of bacteriophage ϕ 29 of *B. subtilis* mediates DNA packaging of ϕ 29 proheads assembled in *E. coli*. Virology **185**:395–400.
 22. Guo, P., and M. Trottier. 1994. Biological and biochemical properties of the small viral RNA (pRNA) essential for the packaging of the double-stranded DNA of phage ϕ 29. Semin. Virol. **5**:27–37.
 23. Hagen, E. W., B. E. Reilly, M. E. Tosi, and D. L. Anderson. 1976. Analysis of gene function of bacteriophage ϕ 29 of *Bacillus subtilis*: identification of cistrons essential for viral assembly. J. Virol. **19**:510–517.
 24. Hendrix, R. W., and R. L. Garcea. 1994. Capsid assembly of dsDNA viruses. Semin. Virol. **5**:15–26.
 25. Ibanez, C., J. A. Garcia, J. L. Carrascosa, and M. Salas. 1984. Overproduction and purification of the connector protein of *Bacillus subtilis* phage ϕ 29. Nucleic Acids Res. **12**:2351–2365.
 26. Karacostas, V., K. Nagashima, M. A. Gonda, and B. Moss. 1989. Human immunodeficiency virus-like particles produced by a vaccinia virus expression vector. Proc. Natl. Acad. Sci. USA **86**:8964–8967.
 27. Kellenberger, E. 1990. Form determination of the heads of bacteriophages. Eur. J. Biochem. **190**:233–248.
 28. Kikuchi, Y., and J. King. 1975. Genetic control of bacteriophage T4 baseplate morphogenesis. III. Formation of the central plug and overall assembly pathway. J. Mol. Biol. **99**:673–716.
 29. Kikuchi, Y., and J. King. 1975. Genetic control of bacteriophage T4 baseplate morphogenesis. I. Sequential assembly of the major precursor, *in vivo* and *in vitro*. J. Mol. Biol. **99**:645–672.
 30. Kikuchi, Y., and J. King. 1975. Genetic control of bacteriophage T4 baseplate morphogenesis. II. Mutants unable to form the central part of the baseplate. J. Mol. Biol. **99**:673–694.
 31. Ladin, B. F., M. L. Blankenship, and T. Ben-Porat. 1980. Replication of herpesvirus DNA. V. Maturation of concatemeric DNA of pseudorabies virus to genome length is related to capsid formation. J. Virol. **33**:1151–1164.
 32. Lee, C. S., and P. Guo. 1994. A highly sensitive system for the assay of *in vitro* viral assembly of bacteriophage ϕ 29 of *Bacillus subtilis*. Virology **202**:1039–1042.
 33. Lee, C.-S., and P. Guo. 1995. *In vitro* assembly of infectious virions of double-stranded DNA phage ϕ 29 from cloned gene products and synthetic nucleic acids. J. Virol. **69**:5018–5023.
 34. Mesyanzhinov, V. V., B. N. Sobolev, E. I. Marusich, A. G. Prilipov, and V. P. Efimov. 1990. A proposed structure of bacteriophage T4 gene product 22—a major prohead scaffolding core protein. J. Struct. Biol. **104**:24–31.
 35. Michaud, G., A. Zachary, B. Rao, and L. Black. 1989. Membrane-associated assembly of a phage T4 DNA entrance vertex structure studied with expression vectors. J. Mol. Biol. **209**:667–681.
 36. Murialdo, H., and A. Becker. 1978. Head morphogenesis of complex double-stranded deoxyribonucleic acid bacteriophages. Microbiol. Rev. **42**:529–576.
 37. Murialdo, H., and A. Becker. 1978. A genetic analysis of bacteriophage lambda prohead assembly *in vitro*. J. Mol. Biol. **125**:57–74.
 38. Nelson, R. A., B. E. Reilly, and D. L. Anderson. 1976. Morphogenesis of bacteriophage ϕ 29 of *Bacillus subtilis*: preliminary isolation and characterization of intermediate particles of the assembly pathway. J. Virol. **19**:518–532.
 39. Newcomb, W. W., and J. C. Brown. 1991. Structure of the herpes simplex virus capsid: effects of extraction with guanidine hydrochloride and partial reconstitution of extracted capsids. J. Virol. **65**:613–620.
 40. Prevelige, P., D. Thomas, and J. King. 1988. Scaffolding protein regulates the polymerization of P22 subunits into icosahedral shells *in vitro*. J. Mol. Biol. **202**:743–757.
 41. Rajagopal, B. S., B. E. Reilly, and D. L. Anderson. 1993. *Bacillus subtilis* mutants defective in bacteriophage ϕ 29 head assembly. J. Bacteriol. **175**:2357–2362.
 42. Reilly, B. E., R. A. Nelson, and D. L. Anderson. 1977. Morphogenesis of bacteriophage ϕ 29 of *Bacillus subtilis*: mapping and functional analysis of the head fiber gene. J. Virol. **24**:363–377.
 43. Rosenberg, A. H., B. N. Lade, D. S. Chui, S. W. Lin, J. J. Dunn, and F. W. Studier. 1987. Vectors for selective expression of cloned DNAs by T7 RNA polymerase. Gene **56**:125–135.
 44. Six, E. W., M. G. Sunshine, J. Williams, E. Haggard-Ljungquist, and B. H. Lindqvist. 1991. Morphopoietic switch mutations of bacteriophage P2. Virology **182**:34–46.
 45. Tosi, M. E., B. E. Reilly, and D. L. Anderson. 1975. Morphogenesis of bacteriophage ϕ 29 of *Bacillus subtilis*: cleavage and assembly of the neck appendage protein. J. Virol. **16**:1282–1295.
 46. Traub, F., B. Keller, A. Kuhn, and M. Maeder. 1984. Isolation of the prohead core of bacteriophage T4 after cross-linking and determination of protein composition. J. Virol. **49**:902–908.
 47. Traub, F., and M. Maeder. 1984. Formation of the prohead core of bacteriophage T4 *in vivo*. J. Virol. **49**:892–901.
 48. Trottier, M., C. L. Zhang, and P. Guo. A new strategy for complete inhibition of viral replication *in vivo* with mutant RNA essential for phage ϕ 29 DNA packaging. Submitted for publication.
 49. Wichitwechkarn, J., S. Bailey, J. W. Bodley, and D. Anderson. 1989. Prohead RNA of bacteriophage ϕ 29: size, stoichiometry and biological activity. Nucleic Acids Res. **17**:3459–3468.
 50. Williams, R., and K. Richards. 1974. Capsid structure of bacteriophage lambda. J. Mol. Biol. **88**:547–550.
 51. Yang, J. T., C.-S. C. Wu, and H. M. Martinez. 1986. Calculation of protein conformation from circular dichroism. Methods Enzymol. **130**:208–269.
 52. Zhang, C. L., K. Garver, and P. Guo. Inhibition of phage ϕ 29 assembly by antisense oligonucleotides targeting viral pRNA essential for DNA packaging. Virology, in press.
 53. Zhang, C. L., C.-S. Lee, and P. Guo. 1994. The proximate 5' and 3' ends of the 120-base viral RNA (pRNA) are crucial for the packaging of bacteriophage ϕ 29 DNA. Virology **201**:77–85.
 54. Zhang, C. L., M. Trottier, and P. X. Guo. 1995. Circularly permuted viral pRNA active and specific in the packaging of bacteriophage ϕ 29 DNA. Virology **207**:442–451.
 55. Zlotnick, A. 1994. To build a virus capsid: an equilibrium model of the self assembly of polyhedral protein complexes. J. Mol. Biol. **241**:59–67.